

## **MODE I FRACTURE BEHAVIOR OF NATURAL FIBER REINFORCED CONCRETE**

S. Ishiguro  
Faculty of Bioresources, Mie University, Tsu, Japan

### **Abstract**

The load-displacement diagrams of sisal fiber reinforced concrete (0.38%, 0.76% and 1.14% v/v of 30 mm long sisal fibers), were determined by notched cubic specimens and wedge splitting procedures. From the load-displacement diagrams, the fracture mechanics properties and softening diagrams were derived. Softening diagrams derived using the polylinear approximation analysis method for sisal fiber reinforced concrete are presented and compared to those of an unreinforced control concrete. The observed differences in fracture behavior between sisal and steel fiber reinforced concretes are also analyzed and discussed.

**Key words:** Fiber reinforced concrete, softening diagram, natural fiber

### **1 Introduction**

Natural organic fibers are produced in large quantities in many countries of the world. Sisal fiber is one of the most useful natural organic fibers, finding application in the production of ropes, fabrics and cleaning pads. Sisal fibers have high tensile strength and are therefore a likely candidate for use in reinforcing concrete. The properties of low-cost natural-fiber reinforced concrete have been investigated by many researchers and these studies have been summarized in state-of-the-art reviews by Swamy (1988),

and Aziz (1981). Many interesting aspects of natural fiber reinforced concrete techniques and technology are discussed at length in these reviews and in their referenced papers. Studies have also been made of the mechanical properties and durability of mortar reinforced with natural agave fibers, widely available in Mexico (Castro et al., 1981). The mechanical properties and durability of natural-fiber reinforced concrete have been investigated (Gram et al., 1987; Aziz et al., 1987) but its fracture mechanics properties have not. The present study is therefore focused on quantifying the fracture mechanics properties of sisal fiber reinforced concrete. To this end, the fracture properties of sisal and steel fiber reinforced concretes were characterized with the aid of a wedge splitting technique, and the properties of the two concretes were compared.

## 2 Experiments

### 2.1 Testing method

Cubic specimens with natural or steel fibers were tested using the simple wedge-splitting procedure described by Tschegg (1990, 1991). A schematic of this testing method is shown in Fig. 1. A cubic specimen is placed on a narrow linear support in a compression-testing machine. A wedge splitting apparatus (consisting of a wedge and load transmission pieces) is placed into the groove of the specimen with a starter notch at the bottom of this groove. The wedge, starter notch, and linear support are vertically aligned allowing the load to be transmitted directly from the testing machine to the specimen, without producing any additional lateral loads or moments.

The wedge transmits a force ( $F_m$ ) from the testing machine to the specimen. The slender wedge transforms this into a large horizontal force component ( $F_h$ ) and a small vertical component ( $F_v$ ) which are applied to the specimen (see Fig.1(b)). The large horizontal component splits the specimen in a manner similar to that of a bending test. The total force ( $F_m$ ) is measured by a load cell in the testing machine. Knowing the wedge angle ( $\alpha$ ) and the total force, the horizontal component ( $F_h$ ) may be easily calculated. The small wedge angle yields vertical forces small enough to be considered negligible. Friction forces between the wedge and load transmission pieces are minimized by the use of rollers. The resulting rolling resistances are small enough to be neglected.

The displacement ( $\delta$ ) of the specimen (referred to as "CMOD", crack mouth opening displacement) is measured at each end of the groove using a clip gage. The two measurements of  $\delta$  serve two purposes: to reduce uncertainty through the use of mean values, and to confirm that the crack propagated parallel to the starter notch in the direction of the linear support. If these values were found to differ by more than 10 %, then the results of a

particular specimen test were considered invalid.

Force ( $F_m$ ) and the two end displacements ( $\delta_1$  and  $\delta_2$ ) were recorded by an electronic data logger. This data was then analyzed to produce a load-displacement curve ( $F_h$ - $\delta$  curve). This load-displacement graph characterizes the fracture properties of the specimen. The area under the  $F_h$ - $\delta$  curve represents the energy needed to fracture the specimen (fracture energy). The specific fracture energy ( $G_f$ ) is a measure of the crack growth resistance of the material and is defined as the ratio of fracture energy to fracture area, normal to the wedge penetration direction. The maximum load in the load-displacement diagram ( $F_{hmax}$ ) may be used to calculate a conventional notch tensile strength. Details on the evaluation and handling of the wedge splitting test data have been described by Tschegg (1991).

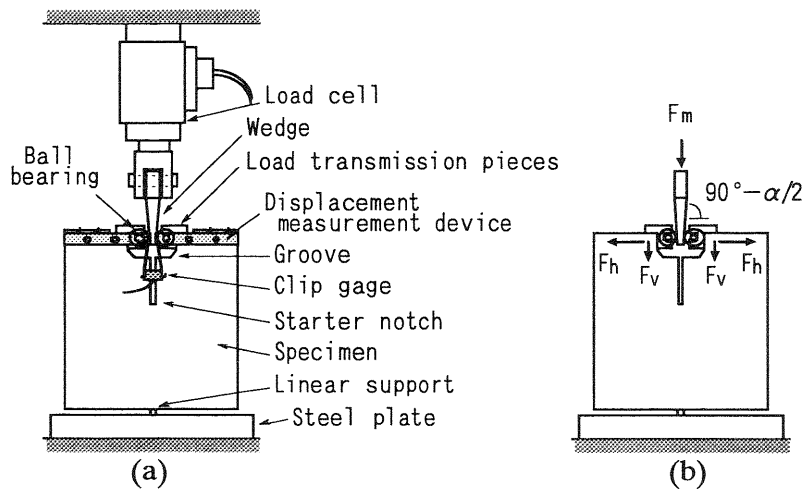


Fig. 1. Wedge-splitting method according to Tschegg (1991)

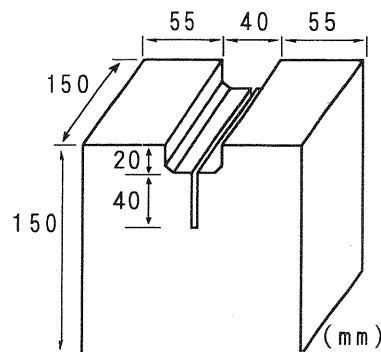


Fig. 2. Size and shape of the specimen

## 2.2 Specimen, material and experimental details

The specimen shape and dimensions used in this study are shown in Fig.2. The rectangular groove with haunches was formed during the casting procedure, while the starter notch (2.0 mm kerf) was cut into the root of the groove with a stone saw shortly before testing.

Table 1. Mixing ratio of control concrete

Sign	Water (kg/m <sup>3</sup> )	Cement (kg/m <sup>3</sup> )	W/C ratio	Sand (kg/m <sup>3</sup> )	Gravel (kg/m <sup>3</sup> )	S.P. (kg/m <sup>3</sup> )	Dmax (mm)
BA	168	280	0.6	808	1016	1.12	20

Table 2. Measured concrete properties

Sign	Fiber type	Fiber length (mm)	Fiber content <sup>1</sup> (%)		Comp. strength (MPa)	Tensile strength (MPa)	Modulus of elasticity (GPa)
			Wf	Vf			
BA	---	---	---	---	20.2	2.18	23.6
SI1%	Sisal	30	1.0	0.38	22.6	2.36	22.8
2%	Sisal	30	2.0	0.76	22.1	2.43	21.9
3%	Sisal	30	3.0	1.14	23.3	2.30	21.0
ST0.5%	Steel	30	14	0.5	22.1	2.65	24.0
1%	Steel	30	28	1.0	25.6	3.08	23.4

<sup>1</sup> Wf: percent weight of cement, Vf: volume fraction of fibers.

Three types of concrete were studied:

- Control concrete without fibers (designated BA): mix ratio of concrete is shown in Table 1. Compressive strength, tensile strength, and modulus of elasticity are listed in Table 2.
- Concrete reinforced with sisal fibers: 1, 2 and 3 % w/w fibers (0.38 %, 0.76 % and 1.14 % v/v respectively) were added to the control concrete (designated SI1%, SI2% and SI3% respectively). The mechanical properties of these concretes are summarized in Table 2. 30 mm long sisal fibers were used in this study. The specific gravity of the fibers is 1.22. The water absorption relative to weight of dry fibers is 66%. Therefore, 66 % w/w water was added to the dry fibers 24 hours before they were mixed into the cement. This water has not been considered in the calculation of w/c values.

3. Concrete reinforced with steel fiber: 0.5 and 1 % v/v of steel fibers were added to the control concrete (designated ST0.5% and ST1% respectively). The mechanical properties of this concrete are summarized in Table 2. The indented steel fibers used for this study were 0.5x0.5 mm in cross-section and 30 mm in length.

After casting, the specimens were allowed to harden for 24 hours. Once set, the specimens were removed from their molds and stored in water for 28 days before testing.

Tests were performed with a mechanical compression testing machine with a load capacity of 9.8 kN using a cross-head velocity of 1 mm/min for each test. All testing was carried out at 20°C using three identical specimens of each material to obtain enough data for a statistical evaluation.

### 3 Results and analysis

The measured load-displacement curves of all test specimens are plotted in Fig. 3. The experimental results of  $F_{hmax}$ -values and fracture toughness ratio ( $W/W_{BA}$ ) are summarized in Table 3. In this ratio,  $W$  is the fracture toughness of fiber reinforced concrete and is defined as the area below the load-displacement curve up to a CMOD of 1.5 mm.  $W_{BA}$  is the area below the load-displacement curve for the unreinforced concrete (BA) up to a zero load. The specific fracture energy  $G_f$  of BA is 100 N/m. Comparing the maximum load ( $F_{hmax}$ ) of the control (BA) to those of the fiber reinforced concretes yields the following values:

$$\begin{aligned} F_{hmax} (S11\%) / F_{hmax} (BA) &= 1.00 \\ F_{hmax} (S12\%) / F_{hmax} (BA) &= 1.01 \\ F_{hmax} (S13\%) / F_{hmax} (BA) &= 1.02 \\ F_{hmax} (ST0.5\%) / F_{hmax} (BA) &= 1.32 \\ F_{hmax} (ST1\%) / F_{hmax} (BA) &= 1.73 \end{aligned}$$

Table 3. Experimental results of maximum load and fracture toughness

Sign	Ligament length (mm)	Specimen width (mm)	$F_{hmax}$ (kN)	Fracture toughness ratio ( $W/W_{BA}$ )
BA	90	150	5.11	1.00
S11%	90	150	5.11	1.65
	90	150	5.15	2.05
	90	150	5.20	2.58
ST0.5%	90	150	6.74	4.50
	90	150	8.86	7.59

These results show that the maximum load ( $F_{hmax}$ ) of sisal fiber reinforced concrete is not significantly affected by the volume fraction of the fibers. On the other hand, the  $F_{hmax}$  of the steel fiber reinforced concretes significantly increased with an increased volume fraction of fibers.

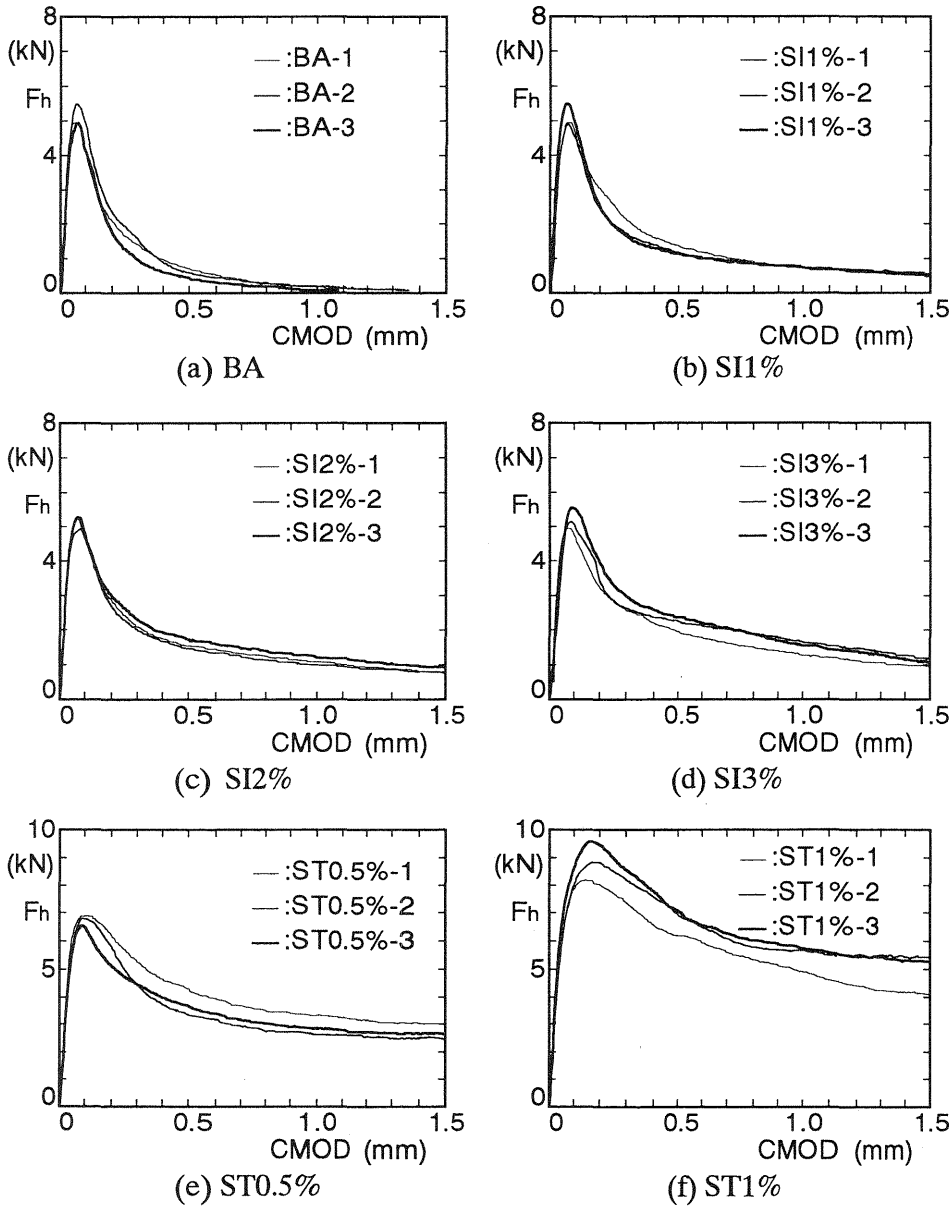


Fig. 3. Measured load ( $F_h$ )-displacement (CMOD) curves

The fracture toughness ratios of sisal fiber reinforced concrete given in Table 3 show that the sisal fiber tested in this study has a good reinforcing efficacy. However, the fracture toughness ratio  $W/W_{BA}$  of SI3%--the highest volume fraction of sisal fibers in this study--is only 57 % of the value for ST0.5%. This means that the resistance of sisal fiber reinforced concrete to crack growth is significantly lower than that of steel fiber reinforced concrete.

In order to fully characterize the fracture behavior of concrete, the strain softening behavior must also be determined. This characteristic is derived from a polylinear softening diagram. In this study, it was determined by a polylinear approximation analysis (Kitsutaka, 1995; Kitsutaka, 1997) of the experimentally measured load-displacement diagrams. The polylinear approximation analysis method is based on finite element methods applied using the fictitious crack model (Uchida et al., 1995). The characteristic values of the polylinear softening diagram are obtained by using an iterative best-fit procedure to match the calculated and measured load-displacement curves (Kurihara et al., 1997). The tolerance used for the fitting procedure was an  $F_{hcal}/F_{hmeas}$  ratio between 0.999-1.001 ( $\pm 0.1\%$ ). Measured and calculated load-displacement curves are shown in Fig. 4 for BA, SI1%, SI2%, SI3% and ST0.5%. This figure shows good agreement between the measured and calculated load-displacement curves. Fig. 5 shows the polylinear softening curves of the concrete specimens. The polylinear softening characteristics are crucial in generating accurate FEM predictions of the effect of geometry on the fracture properties of the material.

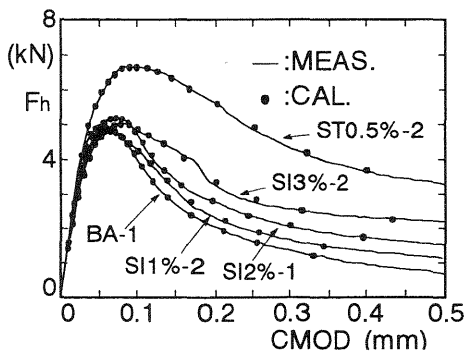


Fig. 4. Measured and calculated load-displacement curves

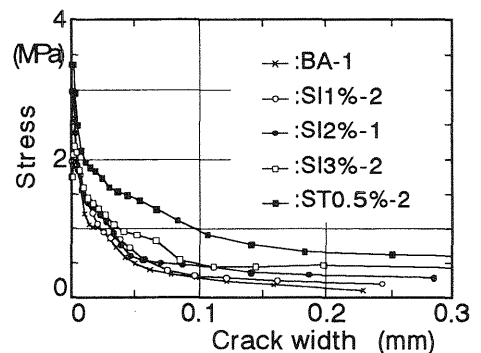


Fig. 5. Polylinear softening curves of typical concrete specimens

The polylinear softening curves of the BA, SI1%, SI2%, SI3%, ST0.5% and ST1% concrete specimens are plotted in Fig. 6. The tensile strength values of the basic (BA) and fiber reinforced concretes, as calculated by best fit, are slightly higher than those determined using cylindrical specimens. The tension softening curves in Fig. 6 clearly show that the

cohesive stress of sisal fiber reinforced concrete at the lower part of the curves is higher than that of BA. This means that sisal fiber reinforced concrete has a higher resistance to crack growth than the unreinforced concrete, as a result of fiber bridging. This leads to increased fracture toughness values for sisal fiber reinforced concrete.

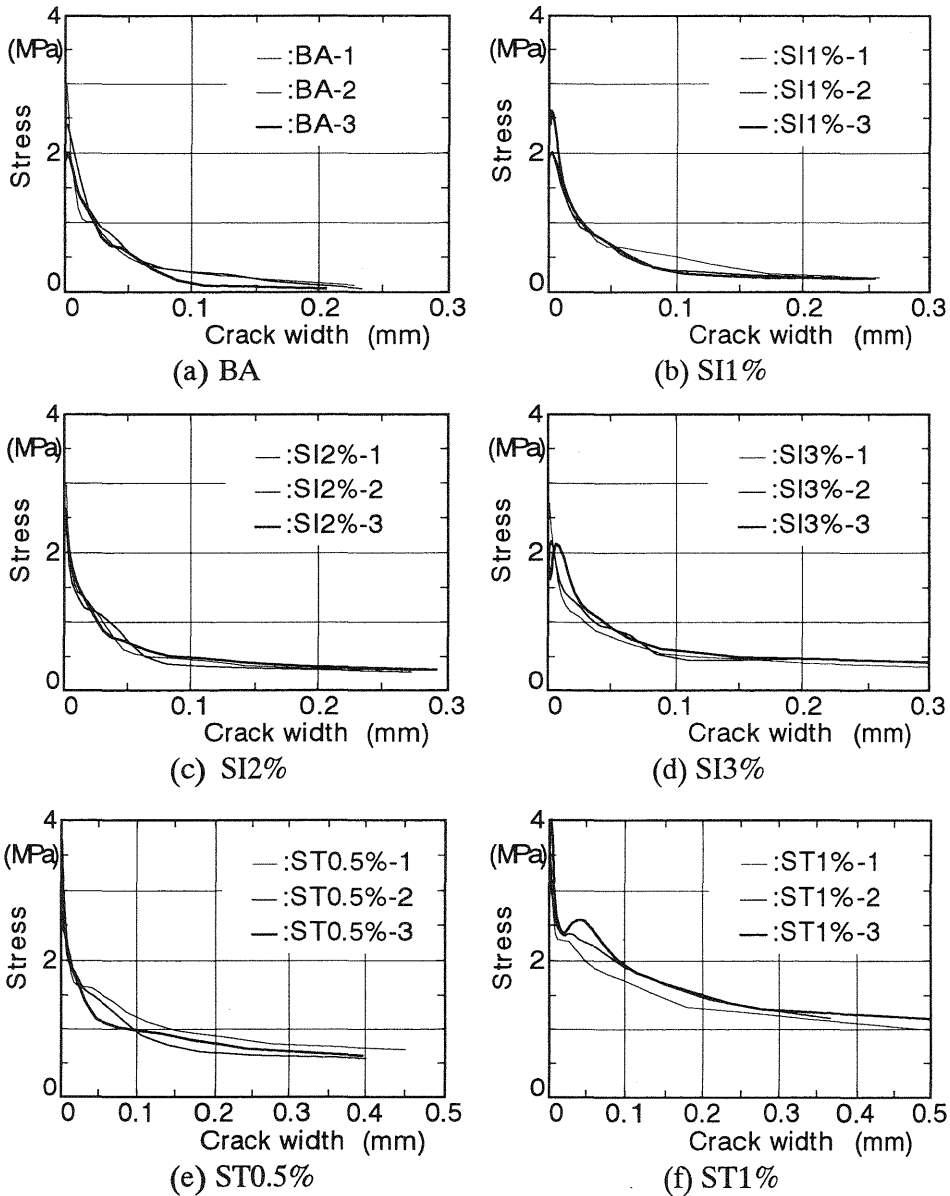


Fig. 6. Determined polylinear softening curves

## 4 Conclusions

Wedge splitting procedures were applied to determine the load-displacement diagrams of sisal and steel fiber reinforced concrete. Softening diagrams were derived from the load-displacement diagrams using the polylinear approximation analysis method. The following conclusions were drawn:

1. The polylinear approximation analysis method (Kitsutaka, 1995; Uchida et al., 1995) is very useful in the determination of tension softening diagrams for sisal or steel fiber reinforced concrete.
2. The wedge splitting method using cubic specimens developed by Tschegg (1991) is appropriate to characterize the fracture behavior of sisal fiber reinforced concrete.
3. The maximum load ( $F_{hmax}$ ) of sisal fiber reinforced concrete is not significantly affected by the volume fraction of the fibers over the range examined in this study (0.38-1.14%). The tension softening diagrams of sisal fiber reinforced concrete indicated that the resistance to crack growth of these concretes increased with increasing fiber content as a result of fiber bridging.
4. The resistance of the steel fiber reinforced concrete to crack growth is considerably higher than that of the sisal fiber reinforced concrete.

## 5 Acknowledgments

The author would like to thank Mr. M. Wada for his assistance with the experiments. He also gratefully acknowledges the inspiration of Dr. E. K. Tschegg, Professor of the Institute of Applied and Technical Physics, Technical University, Vienna, for his originality and experience in wedge splitting test methods.

## 6 References

- Aziz, M.A., Paramasivam, P. and Lee, S.L. (1981) Prospects for natural fibre reinforced concretes in construction. **International Journal of Cement Composites and Lightweight Concrete**, 3(2), 123-132.
- Aziz, M.A., Paramasivam, P. and Lee, S.L. (1987) Natural fibre reinforced concretes in low-cost housing construction. **Journal of Ferrocement**, 17(3), 231-240.

- Castro, J. and Naaman, A.E. (1981) Cement mortar reinforced with natural fibers. **ACI Journal**, 78, 69-78.
- Gram, H.E. and Nimityongskul, P. (1987) Durability of natural fibres in cement-based roofing sheets. **Journal of Ferrocement**, 17(4), 321-327.
- Kitsutaka, Y. (1995) Fracture parameters for concrete based on poly-linear approximation analysis of tension softening diagram, in **Fracture Mechanics of Concrete Structures** (ed F.H. Wittmann), AEDIFICATIO Publishers, 199-208.
- Kitsutaka, Y. (1997) Fracture parameters by polylinear tension-softening analysis. **Journal of Engineering Mechanics**, 123(5), 444-450.
- Kurihara, N., Ando, T., Kunieda, M., Uchida, Y. and Rokugo, K. (1996) Determination of tension softening diagrams of concrete by poly-linear approximation analysis and flexural failure behavior of fiber reinforced concrete. **Proc. Japan Soc. Civil Eng.**, 30(532), 119-129. (in Japanese)
- Swamy, R.N. (1988) Natural fibre reinforced cement and concrete, in **Concrete Technology and Design** (ed R.N. Swamy), 5, Blackie, Glasgow and London.
- Tschegg, E.K. (1990) Load transmission equipment for fracture tests (in German). Patent AT-396997.
- Tschegg, E.K. (1991) New equipment for fracture tests on concrete. **Material Testing**, 33, 338-343.
- Uchida, Y., Kurihara, N., Rokugo, K. and Koyanagi, W. (1995) Determination of tension softening diagrams of various kinds of concrete by means of numerical analysis, in **Fracture Mechanics of Concrete Structures** (ed F.H. Wittmann), AEDIFICATIO Publishers, 17-30.